Journal of Nuclear Materials 405 (2010) 252–260

Contents lists available at ScienceDirect

Journal of Nuclear Materials

journal homepage: www.elsevier.com/locate/jnucmat

On the solution and migration of single Xe atoms in uranium dioxide – An interatomic potentials study

K. Govers *, S.E. Lemehov, M. Verwerft

Belgian Nuclear Research Center (SCK·CEN), Institute for Nuclear Materials Sciences, Boeretang 200, B-2400 Mol, Belgium

ARTICLE INFO

Article history:
Received 3 June 2010
Accepted 13 August 2010

ABSTRACT

Atomic scale simulation techniques based on empirical potentials have been considered in the present work to get insight on the behaviour of single Xe atoms in the uranium dioxide matrix. In view of the high activation energies commonly observed for Xe migration, this work has focused on the so-called "static calculations" (i.e. energy minimization based calculation) of incorporation and migration energies of Xe in UO_2, using empirical interatomic potentials to describe atom interactions. A detailed study of these results enables to determine the solution and the migration properties of Xe in the different stoichiometry regimes, and can be applied as well for the in-pile behaviour of xenon.

1. Introduction

The major role of fission gases behaviour with regards to the nuclear fuel performance under irradiation, and more particularly their release from the matrix, has become an evidence and is clearly illustrated by the numerous publications on the subject (e.g. [1–7]). Discussions on the various mechanisms at play in the release of fission gas still continue and the present authors recently published a study on atomic diffusion [8]. In the article, a meticulous assessment of published transmission electron microscopy data sets was made. The in-pile atomic scale diffusion coefficient was derived from an analytical solution of the differential equations describing a growing bubble collecting impurity atoms. The derived activation energy (0.9 eV) was similar to values published by Turnbull [9], but much lower than the values often used and derived from out-of-pile annealing tests (3.9 eV, [6,10]). The results obtained in [8] motivated us to study the problem by performing atomic scale simulations of Xe diffusion, by investigating the possible migration mechanisms and their associated migration energies.

Before tackling the problem of impurity atom behaviour in UO_2, a comparative study of available interatomic potentials has been made [11,12] to assess the applicability of available interatomic potentials to correctly describe in a first time the UO_2 perfect crystal as well as self-defects, before focusing on the insertion of foreign atoms. It showed the limits of the techniques used (static calculations and molecular dynamics), as well as the the way to treat charge compensation [11]. It has also provided results on uranium vacancy migration, which is expected to affect Xe diffusion (e.g. [9,13,14]). This first step was definitively needed in order to strengthen the methodology used in the present work on Xe behaviour, since much less experimental data are available to validate results for xenon.

In the present work, static calculations (based on energy minimization, see the details in Section 2) have been performed to address the migration of Xe atoms in various defect configurations, including valence modification to U atoms in order to simulate partial charge compensation. Static calculations are generally [13,15–18, e.g.] interpreted in terms of insertion energy – energy of the Xe atom in the trap relative to the empty trap energy, which is applicable for virtually infinitely diluted concentration of Xe – and solution energy (that takes into account for the formation energy of the trap in addition to the insertion energy). Although the latter interpretation has to be used in order to determine the thermodynamic equilibrium, its value is actually highly affected by the calculated formation energies of intrinsic defects in UO_2, which present large scatter from one interatomic potential to another one [11]. The experimental determination of these quantities suffer from similar problem.

Our efforts have therefore focused on the separate determination of the different components of the defect energy:

- formation energy of isolated point defects;
- formation energy of intrinsic defects (oxygen Frenkel pair, Schottky defect, small polaron);
- binding energy of the empty trap relative to isolated point defect energies;
- incorporation energy of one Xe atom in the existing trap.

As shown in the present paper (Sections 3 and 4), binding energies of trap and incorporation energy of Xe inside these traps show much less scatter between potentials than the above-mentioned

* Corresponding author. Tel.: +32 14333093.
E-mail address: kgovers@sckcen.be (K. Govers).

0022-3115/$ - see front matter © 2010 Elsevier B.V. All rights reserved.
doi:10.1016/j.jnucmat.2010.08.013

formation energy of intrinsic defects. The migration energy of Xe that has also been evaluated inside the different traps and show the same agreement among the tested potentials.

The methodology used here is therefore fully justified and has enabled us to determine and interpret the stable defect site and the migration mechanism under in-pile conditions (where irradiation rather than thermodynamic equilibrium governs the formation of defects) as well as under thermodynamic equilibrium. The latter case is generally studied in the three stoichiometry domains. The discussion for both regimes can be found in the Section 5 and the concluding Section 7. Moreover, the approach followed enables interested readers to possibly use a different set of data for the intrinsic defect energies, coming e.g. from other sources.

2. Methodology

2.1. Static calculations

Static calculations were performed with the GULP code [19,20], version 1.3. Defect energies were computed using the Mott–Littleton approach described in [11], with a Newton–Raphson energy minimization procedure. Radii of 10 and 20 Å were chosen for the spheres delimiting respectively the region I and region IIa since it offers a good compromise between the computing time and the convergence of the predicted defect energy, as we could observed in [11].

With regard to the migration energy, a constrained minimization, where the relaxation of the migrating atom is constrained in successive planes, has been considered. The migration path was sampled with 10 regularly spaced planes, starting with the configuration calculated at the previous step and slightly displacing the Xe atom to the next plane. The migration energy reported is the maximum energy value over the series of derived configurations. A second technique was used to obtain a second estimation, with the Rational Function Optimiser (RFO) method [19] that had been used in [11] to derive migration energies. The configuration at the middle of the trajectory was taken as a good initial configuration for the saddle point search by the RFO method.

2.2. Interatomic potential selection

Based on a previous study [11,12], three sets of interatomic potentials describing atomic interactions in the host matrix have been selected: Basak potential [21], Jackson_2 [13,15,22] potential and Morelon potential [23] (we use the denomination proposed in Ref. [11]). The detailed description and parametrization of these two potentials can be found in Refs. [11,13,15,21–23]. These sets of potentials showed a good agreement with experiment on defect properties (formation and migration energies, see [11]) and thermal properties (lattice expansion, melting temperature, see [12]), which are essential in view of the calculations presented here. Two of them offer the additional advantage of having been used in previous studies together with Xe atoms: for the Basak potential, a consistent set of potentials has been developed by Geng et al. [24] to include Xe in the matrix (Xe–O, Xe–U and Xe–Xe interactions). For the Jackson potential, Nicoll et al. [13] have reported a consistent set of Xe–host atoms interactions.

The Xe–O and Xe–U interactions developed by Geng et al. have also been used here in combination with the Morelon potential to describe host atoms interactions.

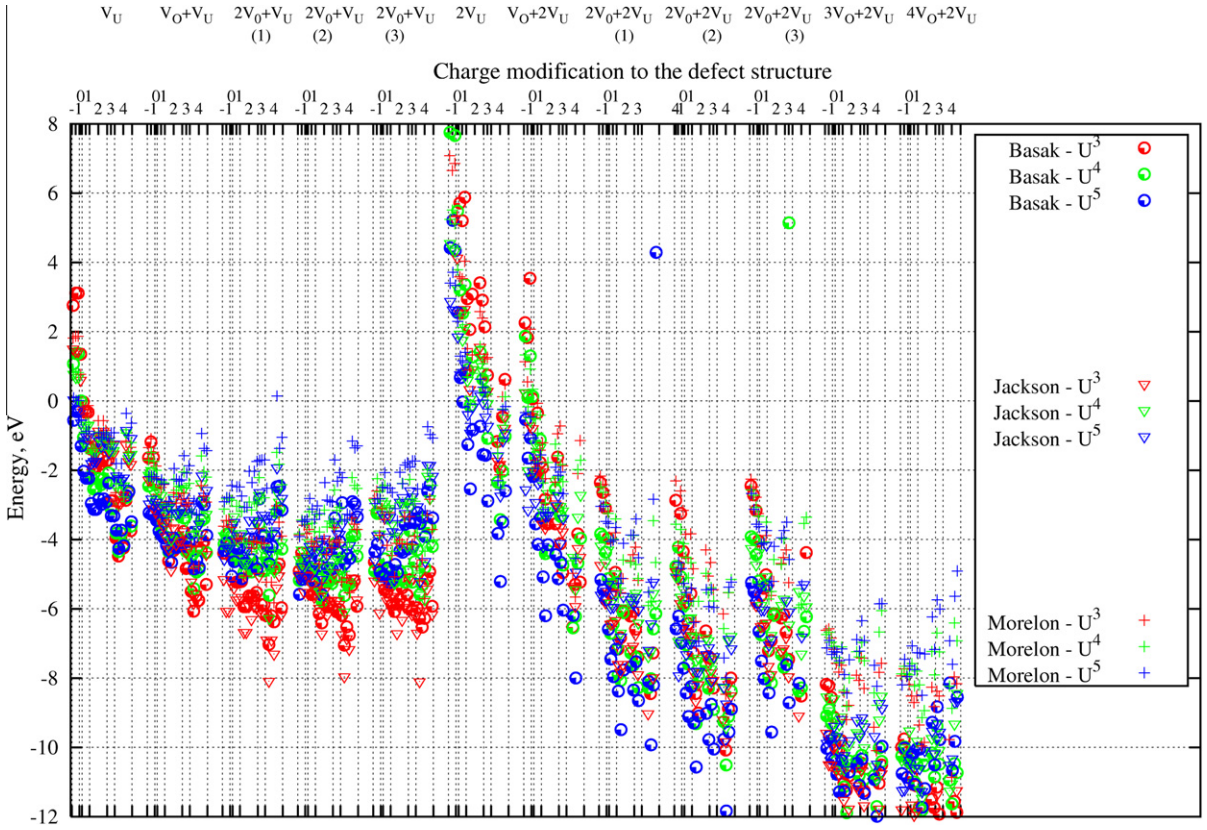

Fig. 1. Binding energy (eV) of various trap sites. For clarity, the traps have been ordered by "type" (corresponding to the number of vacancies present). For each type of vacancy cluster, various charge compensation configuration have been considered, ordered according to the compensation charge they represent. Finally three series of points are represented for each potential, corresponding in each case to the additional substitution of either a U^{3+}, no substitution or substitution of a U^{5+} atom to a regular U^{4+}. The role of this distinction will become more clear in subsequent Figures, where the migration of these atoms will be studied. The same plotting conditions were indeed applied by seek for completeness.

2.3. Charge compensation

Point defects created in empirical interatomic potential studies are generally charged defects, while in the real system, this charge should be somehow compensated to keep it neutral. The oxidation state of uranium is known to be variable and this is reflected in the broad range of non-stoichiometry phases in the U–O system. In stoichiometric $UO_{2.00}$, te uranium cations have an oxidation state 4+ and the oxygen anions −2. At hyperstoichiometry, UO_{2+x}, the excess anions are inserted in interstitial positions and although the oxidation states of the excess anions are not known a priori, experimental data support the assumption that the oxygen anions occupying interstitial positions are doubly charged and that charge compensation is obtained by the oxidation of two cations to the 5+ state [25] or oxidation of one cation to the 6+ state [26].

Direct measurements on the oxidation state of uranium are performed by X-Ray Photoelectron Spectroscopy (XPS) and focus on the line energy and satellites of the core level U4f lines. It should be noted, however, that direct observation of the satellite structure of U^{V} is difficult since it overlaps with the fine structure of U^{IV} and in mixed systems (as is the case in non-stoichiometric UO_{2+x}, a large fraction of the U cations remains in the 4+ oxidation state. Further evidence of the formal oxidation state can be derived from the analysis of the U coordination and the U–O bond lengths. The model proposed by Willis to account for the incorporation of oxygen in the fluorite lattice when hyperstoichiometry develops [27–29] is in line with the oxidation of uranium to the 5+ state. In the present context, we made calculations for defect configuration considering both 5+ and 6+ in case of excess holes. By similarity, in case of excess electrons we will assume a 3+ oxidation state, although no experimental evidence has been found for this (note that experiments in UO_{2-x} are extremely difficult to conduct!).

The interaction parameters for these ions were taken from the work of Jackson et al. [18] where specific interactions for U^{3+}, U^{5+} and U^{6+} with host U^{4+} and O^{2-} ions were developed. For the two other potentials, the short-range potential was not modified in order to simulate charge modifications; only the charge of uranium atoms are modified taking into account the ionicity fraction of the potential (e.g. for Basak potential, the ionicity fraction is 60%, therefore a U^{3+} is handled as having a charge 1.8 instead of 2.4 for the regular U^{4+} ions). The validity of this simple treatment is strengthened by the behaviour, in terms of defect energies, of these potentials compared to the one of Jackson et al.: binding energy of various defect clusters and migration energy inside these clusters have been calculated in the present work and show a similar trend for all tested potentials (see Figs. 1 and 3).

3. Energy properties of various incorporation sites

3.1. Description of the incorporation sites

In previous work on this subject [13,14,30] Xe most stable defect sites are predicted to be uranium vacancies or di- or tri-vacancies. The exact type of defect depends on the stoichiometry, on the Xe concentration and/or on the potential chosen; but in all cases, interstitial positions or substitution on the oxygen sublattice could be excluded. For this reason, only defects containing at least one uranium vacancy are to be considered in the present paper. We will focus on the effect of both uranium or oxygen vacancies and that of modified valence states of uranium atoms on Xe behaviour. To simplify the text, one will make a distinction between

- the defect "type" that only relates to the number and spatial arrangement of the vacancies;
- and the defect "configuration" (or trap) that also includes variations of the basis defect type through modifications of the valence state of surrounding uranium atoms.

The defect types that have been considered consisted of: the isolated V_U, (V_O:V_U), ($2V_O$:V_U) (all three non-equivalent configurations of the oxygen vacancies around the uranium one), ($2V_U$), (V_O:$2V_U$), ($2V_O$:$2V_U$) (3 different configurations), ($3V_O$:$2V_U$), ($4V_O$:$2V_U$).

The charge compensation considered for all these defect types are:

charge = −**1**: $U^{4+} \rightarrow U^{3+}$ (3 configurations);
charge = **0**: no charge compensation;
charge = **1**: $U^{4+} \rightarrow U^{5+}$ (3configurations);
charge = **2**: $U^{4+} \rightarrow U^{6+}$ (3 configurations), $2U^{4+} \rightarrow 2U^{5+}$ (4 configurations);
charge = **3**: $3U^{4+} \rightarrow 3U^{5+}$ (3 configurations);
charge = **4**: $2U^{4+} \rightarrow 2U^{6+}$ (4 configurations), $4U^{4+} \rightarrow 4U^{5+}$ (3 configurations).

An additional charge modification to one of the neighbour uranium atoms has received a specific treatment in our approach by distinguishing it with a different plotting color[1] in the figures. This has been done in order to investigate the behaviour of a *migrating* uranium atom having a modified charge (either a U^{3+}, a U^{4+} or a U^{5+} cation, plotted respectively in red, green and blue). For consistency between the plots and to simplify the treatment of the data, this distinction has been kept in figures reporting binding or incorporation energies. The total charge of each defect is ultimately the combination of the defect type charge, the general charge compensation and the additional charge modification just mentioned. Electroneutrality is globally achieved through charge compensation at larger distance from the defect which therefore do not affect the reported binding or incorporation energies.

3.2. Formation and binding energies of the incorporation sites

As argued in the introduction, the approach followed in this paper will consist of establishing separately the different components of the trap formation energy because of the scatter among potentials on the prediction of intrinsic defect energies.To better illustrate this point, such values are reported in Table 2 for the three potentials considered in the present work.

The (formation) energy of the trap, E_{def}, can be expressed as:

$$E_{def} = E_{form.comp} + E_{binding} \quad (1)$$

where $E_{form.comp}$ the formation energy of the single isolated point defects present in the trap and $E_{binding}$ is the binding energy of the trap. The formation energy (under thermodynamic equilibrium) of single isolated point defects depends, in a close system, on the local equilibrium between the formation of Oxygen Frenkel pairs, Schottky defects and small polarons. The expression for the major single point defects are provided in Table 1 according to the stoichiometry regime.

The binding energies of the different traps are reported in Fig. 1. This figure suggests that neutral defects are favoured, as illustrated by the strong decrease of the binding energy for highly negative defect types (V_U, ($2V_U$), (V_O:$2V_U$)) with increasing charge compensation. Similarly when neutrality is reached, the incorporation of additional charges is not energetically favourable. This trend is clearly illustrated by the behaviour of the red, green and blue re-

[1] For interpretation of color in Figs. 1–7, the reader is referred to the web version of this article.

Table 1
Energies of defects in the different stoichiometry domains as a function of oxygen Frenkel pair (E_{OFP}) and Schottky trio (E_{Sch} formation energies), assuming a point defect model.

Defect	UO_{2-x}	UO_2	UO_{2+x}
V_O	0	$\frac{1}{2} E_{OFP}$	E_{OFP}
O_I	E_{OFP}	$\frac{1}{2} E_{OFP}$	0
V_U	E_{Sch}	$E_{Sch} - E_{OFP}$	$E_{Sch} - 2\ E_{OFP}$

sults, corresponding to the additional charge change to respectively U^{3+}, U^{4+} and U^{5+}, in neutral tri-vacancies defect types. One should recall here that the Fig. 1 is only related to the binding energy of the different clusters and does not include the formation energy of their components.

For the $2V_U$ defect type most configurations are unbound because of the repulsion between both highly negatively charged V_U. This is also true for some of the (V_O:$2V_U$) configurations. One should probably go to larger charge compensations to stabilize these defect.

3.3. Migration energies of uranium vacancies in the various incorporation sites

Considering the expected contribution of the uranium vacancy migration to Xe migration [6,13,14], the V_U migration energy has been calculated for each trap described previously. The calculations have covered the migration of U^{3+}, U^{4+} and U^{5+} into the vacancy site, which is illustrated by different plotting colors in the figures. The migration energy ranges from 2 to 5 eV by the constrained energy method; lower values are predicted for the various $2V_U$ and (V_O:$2V_U$) clusters, however, these clusters were shown to have smaller binding energies or even to be unstable.

The migration energy is clearly lowered by 1 eV in presence of oxygen vacancies and by up to 1.5 eV with two well positioned ones (both along the migration path). It also appears from Fig. 2 that migration into the V_U is easier for a U^{3+} ion, than for a U^{4+}. The U^{5+} has an even larger migration energy. Results obtained with the RFO method show slightly lower migration energy values by about 1 eV, in all cases.

There is a very good agreement between the Basak and the Morelon potential. The Jackson_2 potential predicts slightly lower values, particularly for the U^{3+} migration. Values provided by this potential are very close to zero in some instances, and their validity can be questioned (in other circumstances this potential has shown instabilities for complex defects involving U^{3+} ions [31]).

4. Incorporation energies of a Xe atom in the various traps

4.1. Description of the calculations

A Xe atom was inserted in each defect cluster considered in Section 3. Migration inside these various traps was considered to occur according to the following mechanisms (they are also illustrated on Figs. 3 and 4):

- for defect types containing only one uranium vacancy:
  - the migration of the Xe atom from the vacancy to the nearest interstitial site;
  - the exchange of position between the Xe atom and a regular U atom, whose charge was also varied: U^{3+}, U^{4+} and U^{5+}.
- for defect types containing two uranium vacancies:
  - the migration of the Xe atom between the two uranium vacancies of that defect;

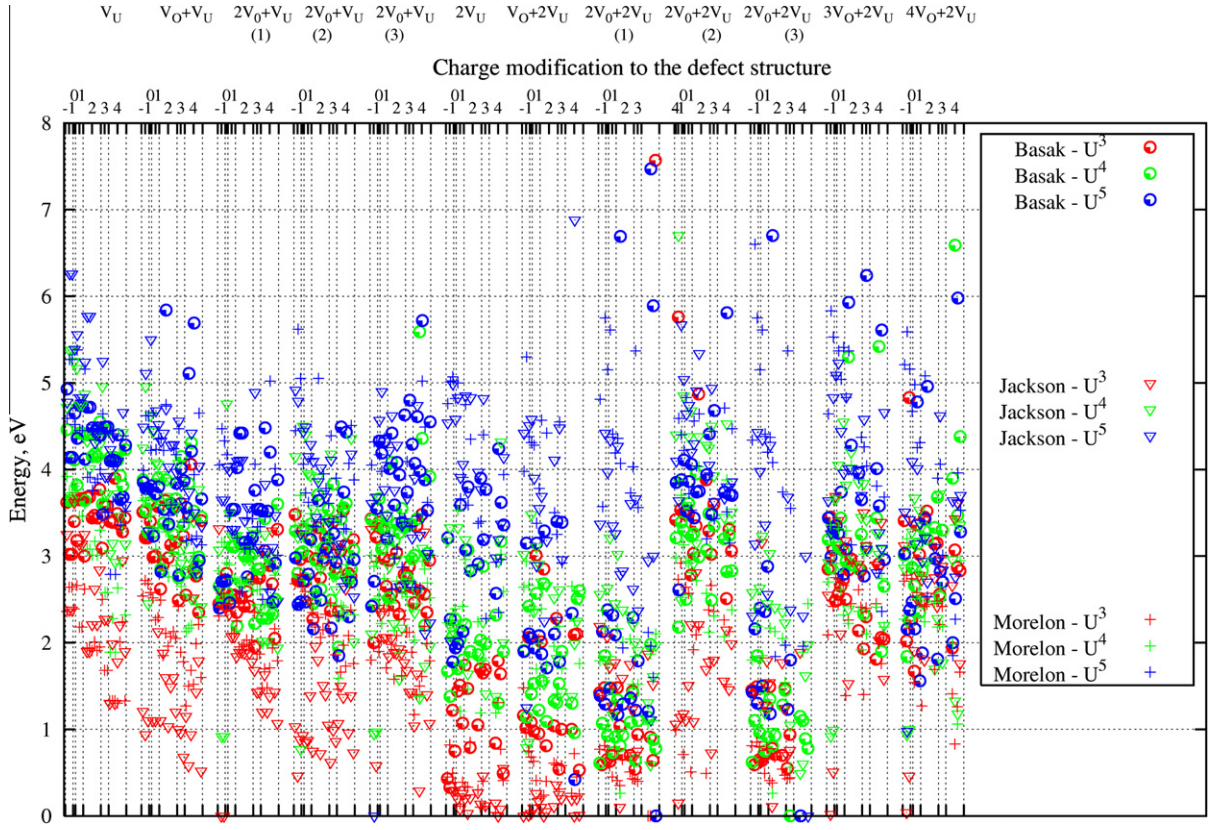

Fig. 2. Migration energy, determined by the constraint minimization technique, of an uranium atom to a vacancy site. Three charges have been considered for the migrating atom, namely 3+ (in red), 4+ (in green) and 5+ (in blue). The axis and legend should be interpreted the same way as for Fig. 1.

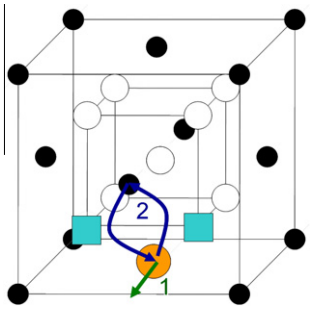

Fig. 3. Illustration of the migration mechanism when the incorporation sites only contains 1 uranium vacancy. The Xe atom is the orange sphere (substitutional position, U atom site), uranium atoms the black ones, oxygen atoms the white ones. The blue squares indicate oxygen vacancies. The first mechanism occurs between the vacant uranium site and an interstitial position; the second one corresponds to the exchange of position of the Xe atom with a regular uranium atom. A similar trend is predicted for all potentials, illustrating the validity of the charge treatment to U atoms for Basak and Morelon potentials.

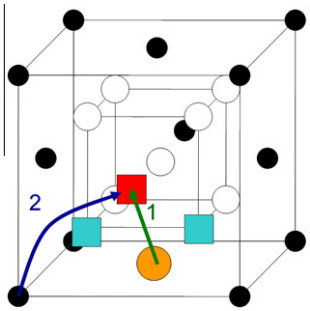

Fig. 4. Illustration of the migration mechanism when the incorporation sites contains 2 uranium vacancies. Same color code as in Fig. 3, the additional red square indicates the (second, since the first one is occupied by the Xe atom) uranium vacancy. The first mechanism occurs between the two vacant uranium sites; the second one corresponds to the migration of a regular uranium atom to the unoccupied site.

– the migration of the uranium vacancy around the Xe atom (between two closest neighbour sites), where the migrating uranium charge was also varied: U^{3+}, U^{4+} and U^{5+}.

The latter type of calculation strictly speaking does not simulate Xe migration but will indicate whether the cluster would migrate as a whole, or whether the migration operates through a cyclic process consisting of clustering with a vacancy, migration through the complex and ending the cycle with the dissociation of the cluster.

This identification is very important because it could strongly affect the dependence of Xe migration with the uranium vacancy concentration, and hence, its modelling in fuel performance codes.

4.2. Incorporation energy

Following the approach presented in the introduction, the incorporation energy of a Xe atom in the defect has been evaluated in this section, i.e. the energy difference between the energy of the Xe inserted in the trap and the energy of the trap itself, assuming the Xe atom is at an infinite distance from the crystal:

$$E_{\text{inc}} = E_{\text{Xeindef}} - \left[E_{\text{def}} + \overbrace{E_{\text{Xe},\infty}}^{=0}\right] \tag{2}$$

where E_{inc} is the incorporation energy of the Xe atom, $E_{\text{Xe in def}}$ the total energy of the system when the Xe atom has been inserted in the trap, E_{def} the formation energy of the trap (without Xe atom) and $E_{\text{Xe},\infty}$ the reference energy of an isolated Xe atom, taken as zero.

The incorporation energy of a Xe atom (see Fig. 5) ranges from 4 to 6 eV in defect types containing only one uranium vacancy. In presence of two uranium vacancies, the incorporation energy is lowered by 1 to 2 eV, and is even lower for the particular configuration $2V_O+2V_U$ (1). This tetra-vacancy consists of two uranium vacancies located at (0,0,0) and $(\frac{1}{2},\frac{1}{2},\frac{1}{2})$; and the closest two oxygen vacancies, at $(\frac{1}{4},\frac{1}{4},\frac{1}{4})$ and $(\frac{1}{4},\frac{1}{4},-\frac{1}{4})$. These coordinates are relative to the conventional unit cell for the fluorite structure. The latter defect presents the lowest incorporation energy, between 1 and 2 eV depending on the charge modification chosen. These results clearly illustrate that Xe needs large defect sites to be accommodated, as also observed in previous studies.

4.3. Migration energies

The migration energies in traps containing only one uranium vacancies are not shown on Figs. 6 and 7 because of their high value, above 8 eV. It means that the migration mechanisms considered, from a vacancy to an interstitial position or the exchange of position with a regular uranium atom will not occur.

In the case of defect types involving two uranium vacancies, the situation is far different. The motion of a Xe atom between two uranium vacancy sites shows a very low migration energy, between 0.3 and 1.5 eV. This is much smaller than the V_U migration energy itself, which confirms that the jumps of uranium vacancies are the rate-determining process for Xe migration.

Another process has been investigated, consisting of the migration of the uranium vacancy in the cluster, "around" the Xe atom. It will indicate whether the cluster would migrate as a whole or rather through a clustering – dissociation process. Our results show that uranium vacancy migration energy is slightly higher around the Xe atom (~4.5 eV) than in the bulk (~3 eV). On the other hand, the presence of Xe in one type of tetravacancy was energetically very favourable (about 2 eV lower than other types of defects). Such defect cluster could then migrate with a similar, or lower, activation energy than uranium vacancies through the UO_2 lattice. Both types of migration processes have therefore to be taken into account to determine which one presents the lowest migration barrier.

5. Xe activation energy in the different stoichiometry regimes

The determination of the activation energies in the different stoichiometry domains is not straightforward from the results of static calculations, since it involves the estimation of different defect formation energies, for which large uncertainties remain. The activation energy E^* is indeed the sum of the migration energy of the rate-determining step (the uranium vacancy migration as suggested by our previous results, in agreement with [6,9,32]) and the energy difference between the trap in which Xe migration occurs and its stable incorporation defect:

$$E^* = E_{\text{mig},V_U} + E_{\text{defect for mig}} - E_{\text{stable def}} \tag{3}$$

The energy of the Xe atom in the different traps can be determined from the formation energy of their components, the binding energy of the defect (without Xe atom) and the incorporation energy of the Xe atom:

$$E_{\text{def}} = E_{\text{form.comp}} + E_{\text{binding}} + E_{\text{Xe inc}} \tag{4}$$

From the latter two equations,

$$E^* = E_{\text{mig},V_U} + \Delta E_{\text{form.comp}} + \Delta E_{\text{binding}} + \Delta E_{\text{Xe inc}} \tag{5}$$

The Δ referring to the difference between the defect in which migration occurs and the stable defect.

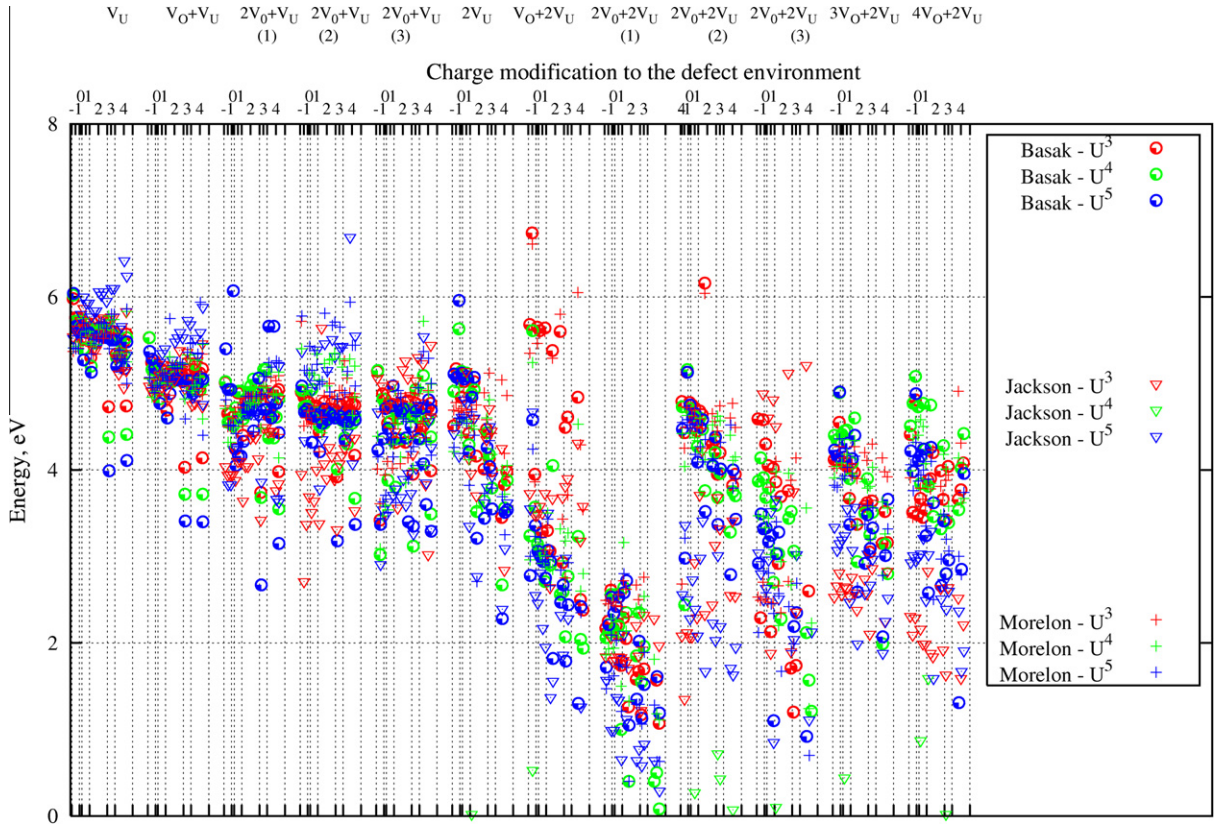

Fig. 5. Incorporation energy of Xe in the various traps. The axis and legend should be interpreted the same way as for Fig. 1.

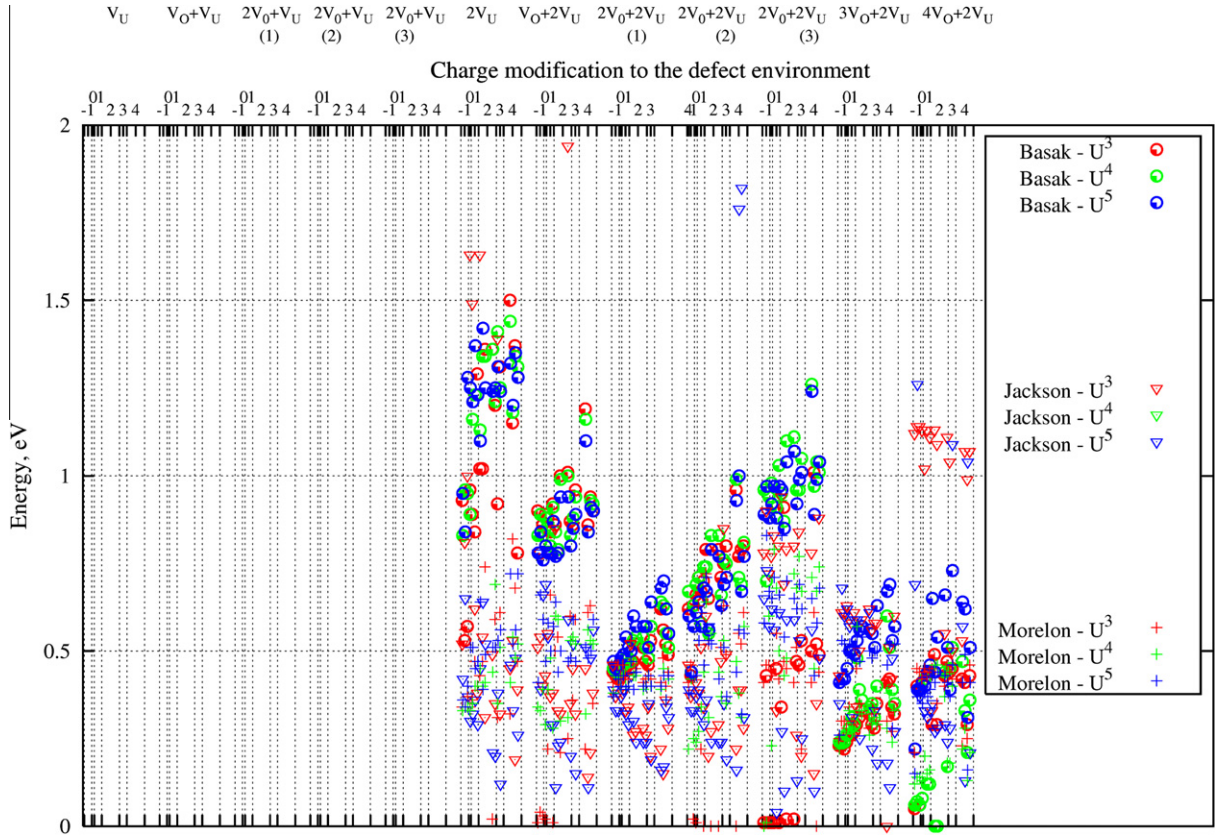

Fig. 6. Migration energy, determined by the constraint minimization technique, in the various traps. Xe migration occurs to the closest interstitial site if only one uranium vacancy is present in the trap; between two uranium vacancy sites when these are present. The axis and legend should be interpreted the same way as for Fig. 1. A similar trend is predicted for all potentials, illustrating the validity of the charge treatment to U atoms for Basak and Morelon potentials.

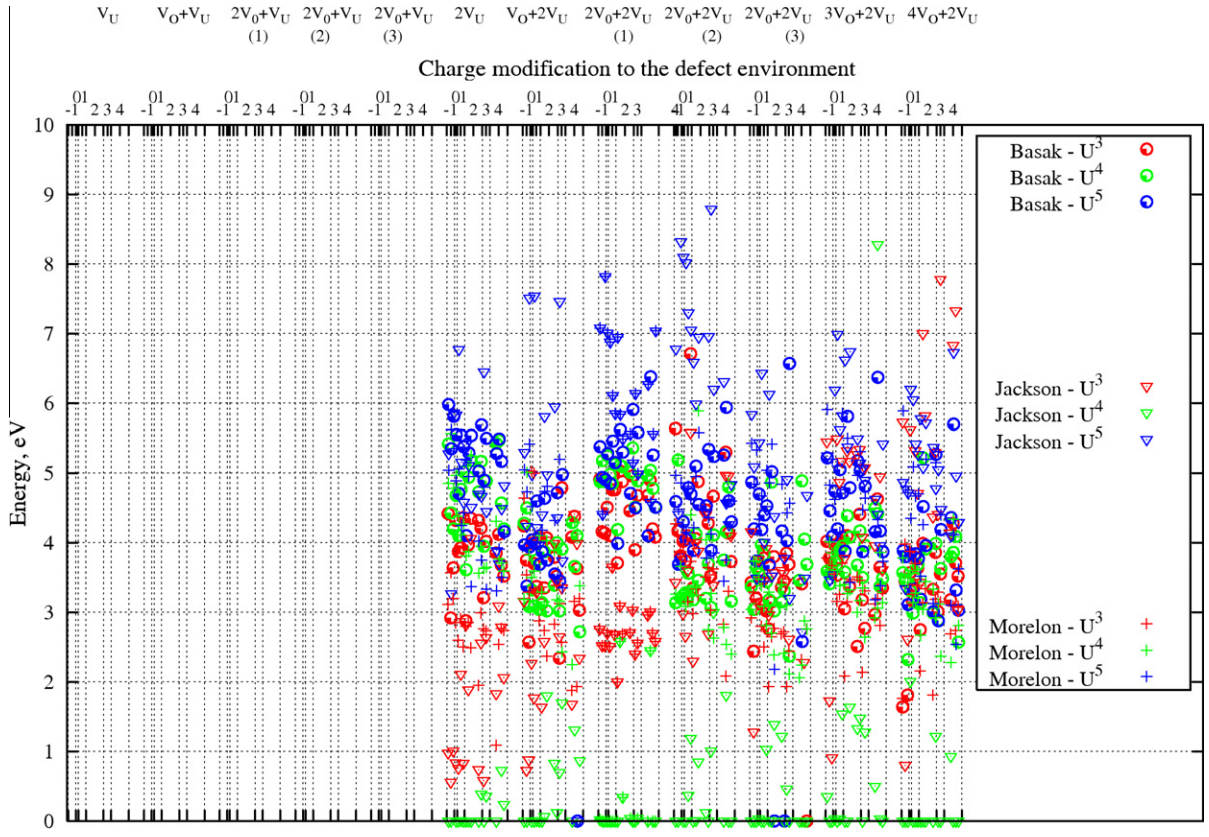

Fig. 7. Migration energy, determined by the constraint minimization technique, in the various traps. The mechanism corresponds to an exchange of Xe and U positions if only one uranium vacancy is present in the trap or to the migration of a uranium vacancy when two V_U are present in the defect. In both cases, three charges have been considered for the migrating atom, namely 3+ (in red), 4+ (in green) and 5+ (in blue).The axis and legend should be interpreted the same way as for Fig. 1.

Formation energies of the components are function of the dominant defect energies, oxygen Frenkel pairs and Schottky trios. The laws of mass actions provide the relations summarized in Table 1.

Binding and incorporation energies can be estimated for various defects from Figs. 1 and 5. Their high (negative) values for the tetravacancy make their creation energetically accessible. Based on the data obtained up to now, the following migration mechanisms can be envisaged, even if the uncertainties, particularly on the oxygen Frenkel pairs and Schottky trios formation energies, impose to take this discussion with caution, since other mechanism could be favoured taking other values:

Hypostoichiometric fuel: Trivacancies are the stable solution site, since many oxygen vacancies are present at no additional cost. Migration occurs for Xe located in tetra-vacancies (rate-determining step: uranium vacancy migration *around* the Xe atom).
Stoichiometric fuel: Different solution sites have a similar (less than 1 eV difference) formation energy and could be envisaged: di-, tri- and tetra-vacancies. The uncertainties on the different parameters do not allow to select the most stable one, but neglecting the difference in binding energy, the activation energy can be approximated by the migration energy of a uranium vacancy *around* the Xe atom.
Hyperstoichiometric fuel: Xe is located at uranium sites (in uranium vacancies). Different migration mechanism can be envisaged, accounting for the fact that the creation of oxygen vacancies is difficult (need to create 1 oxygen Frenkel pair, ~3 eV). The first one is again the migration of tetra-vacancies and the Xe they contain, a second mechanism could be via a $V_O + 2V_U$ defect instead, or, finally, in view of the very low experimental activation energy (1.7 eV [33]) a simple uranium vacancy assisted mechanism.

6. Discussion

6.1. Diffusion in the different stoichiometry domains

Table 3 summarizes the different mechanisms and the associated activation energy. Migration of the Xe atom together with the cluster in which it is located seems to be favourable in hyposto-ichiometric and stoichiometric fuel, because of the high binding energy of the tetravacancy. The activation energies determined agree with the experimental observations of 6.0 eV in UO_{2-x}, and a lower value, 3.9 eV in stoichiometric UO_2 [33]. In hyperstoichiometric fuel a simple vacancy-assisted mechanism has the lowest activation energy, that of uranium vacancy migration: between 2.5 and 3.5 eV according to static calculations (2.4 eV were obtained by MD [31,34], this value is also the one recommended by

Table 2
Energies (in eV) of intrinsic defects in UO_2 for all potentials tested. The first value is for clustered defects, the second one when the components (each single point defect) are not interacting. Polarons, which are intrinsic defects in real system, cannot be treated as such with empirical interatomic potentials: the treatment implies to move 2 regulars atoms "at an infinite distance" from the crystal and reciprocally one U^{3+} and one U^{5+} from there to the crystal. One has then additionally to take into account the 4th and 5th ionization energies of U. For this reason polarons energies will not be reported here.

Defect energy	Basak [21]	Morelon [23]	Jackson [15]
Schottky, $E_{Sch.}$	5.4 eV/10.8 eV	3.9 eV/8.0 eV	5.6 eV/11.1 eV
Oxygen Frenkel pair, E_{OFP}	4.8 eV/6.0 eV	3.0 eV/3.9 eV	3.9 eV/4.9 eV
Uranium Frenkel pair, E_{UFP}	12.4 eV/ 17.0 eV	11.9 eV/ 15.7 eV	14.7 eV/19.2 eV

Table 3
Activation energy for the migration mechanisms in different stoichiometry domains with E_{OFP} = 3 eV, E_{Sch} = 7 eV.

	UO_{2-x}	UO_2	UO_{2+x}
Trap site	Tri-vacancy	Tri-vacancy	V_U
Defect for migration	Tetra-vacancy	Tetra-vacancy	Tetra-vacancy
Rate-determining step	V_U migration in the defect	V_U migration in the defect	V_U migration in the defect
E_{mig}	4.5 eV	4.5 eV	4.5 eV
$\Delta E_{form.\ const.}$	$E_{V_U} = E_{Sch}$	$E_{V_U} = E_{Sch} - E_{OFP}$	$E_{V_U} + 2E_{OFP} = E_{Sch}$
$\Delta E_{binding}$	~−2 eV	~−2 eV	~−4 eV
$\Delta E_{Xe\ incorporation}$	~−2.5 eV	~−2.5 eV	~−2.5 eV
E^*	6.5 eV	~4.0 eV	5 eV
Trap site		Di-vacancy	V_U
Defect for migration		Tetra-vacancy	V_O + 2 V_U
Rate-determining step		V_U migration in the defect	V_U migration in the defect
E_{mig}		4.5 eV	4.5 eV
$\Delta E_{form.\ const.}$		$E_{V_U} + E_{V_O} = E_{Sch} - \frac{1}{2}E_{OFP}$	$E_{V_U} + E_{V_O} = E_{Sch} - E_{OFP}$
$\Delta E_{binding}$		~−2 eV	~−2 eV
$\Delta E_{Xe\ incorporation}$		~−3 eV	~−2 eV
E^*		~5.0 eV	4.5 eV
Trap site		Tetra-vacancy	V_U
Defect for migration		idem	–
Rate-determining step		V_U migration in the defect	V_U migration to the defect
E_{mig}		4.5 eV	2.4 eV
$\Delta E_{form.\ const.}$		0	$E_{V_U} = E_{Sch} - 2E_{OFP}$
$\Delta E_{binding}$		0	–
$\Delta E_{Xe\ incorporation}$		0	–
E^*		4.5 eV	~2.4 eV
Experimental E^*	**6.0 eV**	**3.9 eV**	**1.7 eV**

Turnbull [9]). Experimentally Xe shows a slightly lower activation energy than uranium vacancies, with 1.7 eV.

6.2. In-pile diffusion

Three different regimes are generally observed for the in-pile diffusion of xenon. Athermal diffusion, induced by collisions in displacement cascade events following a fission, provides the major contribution to diffusion at low temperatures (below 1100 K) and will not be discussed further here. The other regimes, for which migration occurs through atomic jumps, are thermally activated and an activation energy can be associated to them. It has been postulated to occur in both cases through a uranium vacancy assisted mechanism [6,8,14,35], where the rate-determining step is the migration of the uranium vacancies. This is in agreement with the results obtained in the present work. The difference between both regimes is that at high temperature (above ~1700 K), the major contribution to the defect population arises from thermal disorder.

In the intermediate temperature domain, one faces a non-equilibrium concentration of (uranium) vacancies induced by the irradiation. The concentration of vacancies results from an equilibration between their production (proportional to the fission rate and independent from the temperature) and their removal at sinks. Considering the increase of their mobility as temperature increases, the efficiency of sinks will be higher, resulting in a *decrease* of the uranium vacancy concentration with temperature. The diffusion coefficient of Xe atoms being proportional to both the uranium vacancy concentration and their mobility, with the consequence that the apparent activation energy is lower than the migration energy. Taking the relations derived in [9,36,37]

$$D_{Xe} = \text{constant} \times \sqrt{\dot{F} \exp\left(\frac{-E_{\ mig,V_U}}{k_B T}\right)} \tag{6}$$

where $\dot{F}$ is the fission rate, and using a uranium vacancy migration energy of 2.4 eV (as derived with MD [31,34] or with static calculations – 2.5 to 3.5 eV, present work –), one observes a very good agreement with the value established in [9,37].

7. Conclusions

Contrarily to the study of helium diffusion [37], molecular dynamics techniques are not an optimal choice for investigating Xe diffusion in a not-too-disturbed UO_2 lattice, nor was Temperature accelerated Dynamics (TAD) [37–40], because of the complexity of the processes at play and of the high activation energy associated to them, implying that enough statistics can only be obtained at very high temperatures where the lattice structure is more and more disturbed (and fully disordered when the melting point is reached). However, Xe migration could still be investigated using energy minimization techniques (static calculations).

In the present study, the components of the activation energy, i.e. the formation energies of isolated defects, the binding energies of traps, the incorporation energy of Xe in those traps and ultimately the migration energy of both Xe atoms and uranium vacancies inside the different traps, have been evaluated for more than 400 types of traps, with three sets of interatomic potentials. The contribution of each term has been considered separately considering that the formation energies of intrinsic defects (Schottky trio and oxygen Frenkel pair) show large scatter among the tested potentials and would induce undue bias to the final results, while a much better agreement is observed for binding and migration energies.

This approach has enabled to derive the activation energy of Xe in the different stoichiometry domains as well as under in-pile conditions. The values derived are in agreement with experimental data or recommendation, except for the activation energy in hyper-stoichiometric fuel, where an overestimation is observed. In this particular stoichiometry domain, the presence of Xe in single uranium vacancies is energetically favourable. The migration mechanism is predicted to occur through jumps between two uranium vacancies, with V_U migration as the rate-determining step, but still overestimate the recommended value. More investigations are needed in that direction, both experimentally and theoretically, to solve this issue. Other migration processes could be operating, in more complex defect structures involving e.g. oxygen interstitials.

For the other domains of stoichiometry, our results indicate a much lower incorporation energy of Xe in one type of tetravacancy

compared to other traps. Considering this, this type of defect could be either the stable defect size in the stoichiometric domain, either constitute a low-populated state that provides the major contribution to Xe migration (hypo-stoichiometric domain). For this type of tetravacancy, migration would occur trough the migration of the whole cluster rather than through a clustering/dissociation process with isolated uranium vacancies.

Acknowledgements

Part of this work was funded by the Université Libre de Bruxelles (ULB) and the SCK·CEN through a PhD grant and by the European Commission through the FP7 F-BRIDGE project (Contract No. 211690).

References

[1] D.R. Olander, Fundamental Aspects of Nuclear Fuel Elements, Technical Information Center, Energy Research and Development Administration, 1976.
[2] D. Olander, D. Wongaswaeng, J. Nucl. Mater. 354 (2006) 94.
[3] H. Matzke, J. Nucl. Mater. 114 (1983) 121.
[4] H. Matzke, Diffusion Processes in Nuclear Fuels, Elsevier Science Publishers, 1992.
[5] P. Lösönen, J. Nucl. Mater. 280 (2000) 56.
[6] H. Matzke, Rad. Eff. 53 (1980) 219.
[7] K. Lassmann, H. Benk, J. Nucl. Mater. 280 (2000) 127.
[8] K. Govers, S. Lemehov, M. Verwerft, J. Nucl. Mater. 374 (2008) 461.
[9] J. Turnbull, C. Friskney, J. Findlay, F. Johnson, A. Walter, J. Nucl. Mater. 107 (1982) 168.
[10] R. Cornell, Philos. Mag. 19 (1969) 539.
[11] K. Govers, S. Lemehov, M. Hou, M. Verwerft, J. Nucl. Mater. 366 (2007) 161.
[12] K. Govers, S. Lemehov, M. Hou, M. Verwerft, J. Nucl. Mater. 378 (2008) 66.
[13] S. Nicoll, H. Matzke, C. Catlow, J. Nucl. Mater. 226 (1995) 51.
[14] C. Catlow, Proc. Roy. Soc. Lond. A 364 (1978) 473.
[15] R. Jackson, C. Catlow, J. Nucl. Mater. 127 (1985) 161.
[16] R. Grimes, Mater. Res. Soc. Symp. Proc. 257 (1992) 361.
[17] R. Grimes, C. Catlow, Philos. Trans. Roy. Soc. Lond. A 335 (1991) 609.
[18] S. Nicoll, H. Matzke, R. Grimes, C. Catlow, J. Nucl. Mater. 240 (1997) 185.
[19] J. Gale, General Utility Lattice Program, version 1.3, IVEC, <http://www.ivec.org/gulp/>.
[20] J. Gale, A. Rohl, Mol. Simul. 29 (2003) 291.
[21] C. Basak, A. Sengupta, H. Kamath, J. Alloys. Compd. 360 (2003) 210.
[22] R. Jackson, C. Catlow, J. Nucl. Mater. 127 (1985) 167.
[23] N.-D. Morelon, D. Ghaleb, J.-M. Delhaye, L.V. Brutzel, Philos. Mag. 83 (2003) 1533.
[24] H. Geng, Y. Chen, Y. Kaneta, M. Kinoshita, Molecular dynamics study on planar clustering of xenon in UO_2, J. Alloys Compd. 457 (2008) 465.
[25] G. Allen, P. Tempest, J. Tyler, Nature 295 (1982) 48.
[26] J. Pireaux, J. Riga, E. Thibaut, C. Tenret-Noël, R. Caudano, J. Verbist, Chem. Phys. 22 (1977) 113.
[27] B. Willis, Proc. Br. Ceram. Soc. 1 (1964) 9.
[28] B. Willis, Acta Cryst. 34 (1977) 88.
[29] A. Murray, B. Willis, J. Solid State Chem. 84.
[30] R. Ball, R. Grimes, J. Chem. Soc. Faraday Trans. 86 (1990) 1257.
[31] K. Govers, Atomic Scale Simulations of Noble Gases Behaviour in Uranium Dioxide, Ph.D. thesis, Université Libre de Bruxelles (ULB), Belgium, 2008. <http://theses.ulb.ac.be/ETD-db/collection/available/ULBetd-06172008-103750/>.
[32] H. Matzke, Diffusion processes in nuclear fuels, J. less-common metals 121.
[33] W. Miekeley, F. Felix, J. Nucl. Mater. 42 (1972) 297.
[34] A. Kupryazhkin, A. Zhiganov, D. Risovany, K. Nekrassov, V. Risovany, V. Golovanov, J. Nucl. Mater. 372 (2008) 233.
[35] J. Turnbull, Radiat. Effects 53 (1980) 243.
[36] J. Sharp, Radiation Enhanced Diffusion, Tech. Rep., AERE Rep. No. 6267 (1969).
[37] K. Govers, S. Lemehov, M. Hou, M. Verwerft, J. Nucl. Mater. 395 (2009) 131.
[38] W. Smith, T. Forester, I. Todorov, THE DL POLY 2 USER MANUAL version 2.18, CSE Department, STFC Daresbury Laboratory, Warrington, UK, 2007.
[39] T. Ichinomiya, B. Uberuaga, K. Sickafus, Y. Nishiura, M. Itakura, Y. Chen, Y. Kaneta, M. Kinoshita, J. Nucl. Mater. 384 (2009) 315.
[40] Y. Shim, G. Amar, B.P. Uberuaga, A.F. Voter, Phys. Rev. B 76 (2007) 205439.